Ergothioneine, a dietary amino acid with a high relevance for the interpretation of label-free surface enhanced Raman scattering (SERS) spectra of many biological samples

Stefano Fornasaro [a], Elisa Gurian [a], Sofia Pagarin [b], Elena Genova [c], Gabriele Stocco [d], Giuliana Decorti [c,e], Valter Sergo [a,f], Alois Bonifacio [a,*]

[a] Raman Spectroscopy Lab, Department of Engineering and Architecture, University of Trieste, 34100 Trieste, Italy
[b] PhD Course in Science of Reproduction and Development, Department of Medical, Surgical and Health Sciences, University of Trieste, 34100 Trieste, Italy
[c] Institute for Maternal and Child Health IRCCS Burlo Garofolo, 34100 Trieste, Italy
[d] Department of Life Sciences, University of Trieste, 34100 Trieste, Italy
[e] Department of Medical, Surgical and Health Sciences, University of Trieste, 34100 Trieste, Italy
[f] Faculty of Health Sciences, University of Macau, SAR Macau

ARTICLE INFO

Keywords:
Ergothioneine
Antioxidant
SERS
Biofluids
Serum
Erythrocytes
Plasma
Raman

ABSTRACT

Intense SERS spectra of the natural amino acid ergothioneine (ERG) are obtained on different substrates upon 785 nm excitation. A characteristic spectral pattern with a distinctive intense band at 480–486 cm^{-1} is conserved when substrates of different type and characteristics are used. On the basis of available literature, we propose ERG is adsorbed on the metal surface in its thiolate form via the sulphur and heterocyclic nitrogen. The same spectral pattern is obtained in SERS spectra of filtered erythrocytes lysates, confirming the presence of ERG in those cells. The occurrence of ERG bands in label-free SERS spectra of serum and plasma reported in literature by different authors is discussed, highlighting the importance of this amino acid for the interpretation of SERS spectra of these biofluids.

1. Introduction

L-(+)-ergothioneine (ERG), first isolated in 1909 from the fungus *Claviceps purpurea* [1], is an unusual dietary amino acid containing the imidazole-2-thione substructure, and a strong antioxidant with a hypothesized physiological role as a vitamin-like compound [2,3]. Although ERG is synthesized only by certain microorganisms, especially fungi and actinobacteria, it is almost ubiquitously found in plants and animals. Plants acquire it via the soil, while animals (and humans) absorb ERG exclusively by dietary sources, mostly the mushrooms *Boletus edulis* and *Pleurotus ostreatus*, oat bran, red and black beans, and organ meat as kidney and liver [4–6]. In humans, ERG is highly absorbed following oral consumption and is not rapidly metabolized or excreted in urine, but accumulates differentially in most cells and tissues in the body, according to their expression of a highly selective transport protein, known as solute carrier family 22, member 4 (SLC22A4), which plays a key role in ERG disposition [3,7]. ERG is mostly present inside erythrocytes in whole blood (with typical values of ~125 μM in whole blood and millimolar levels reported for red blood cells), but some studies have found ERG to be present in other biofluids such as cerebrospinal fluid (with levels around 250 nM), human breast milk and aqueous humor of the eye. A detailed list can be found in [2]. ERG exists in solution as a tautomer between thiol and thione forms (Fig. 1). The long-half life and ability to accumulate in the body are also related to the fact that at physiological pH, the thione tautomer is predominant, giving ERG much greater stability compared to other thiols (e.g. glutathione), due to the unusual resistance to auto-oxidation of the thione form [8].

ERG exhibited a wide range of cytoprotective properties, including the ability to scavenge reactive oxygen and reactive nitrogen species (ROS/RNS), modulate inflammation, protect against UV radiation-induced damage, inhibit myeloperoxidase activity, protect against the phagocyte respiratory burst and promote neuronal differentiation [3]. Many studies in cells, animal models, and also population studies, suggest that the cytoprotective abilities of ET may be helpful against neurologic [9] and cardiovascular [10] disorders, as well as preeclampsia [11],

* Corresponding author.
E-mail address: abonifacio@units.it (A. Bonifacio).

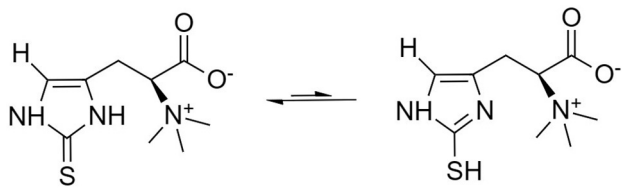

Fig. 1. Chemical structures of the two tautomeric forms of ERG (IUPAC name (2*S*)-3-(2-thioxo2,3-dihydro-1H-imidazol-4-yl)-2-(trimethylammonio)propanoate). The thione (left) is the predominant form at pH 7.4.

ischemia-reperfusion injury [12], and acute respiratory distress syndrome [13]. Interestingly, ERG blood levels decline with age [9], and low plasma levels of ERG have been associated with age-related disorders [14].

Considering the ubiquitous presence of ERG in tissues and biofluids, the goal of the present study is to investigate if this molecule exhibits a SERS spectrum, what its spectral characteristics might be, and if it can be detected in a real biological sample such as lysates of red blood cells, where ERG is known to accumulate. The study also aims at assessing if any spectral feature of ERG can be retrospectively identified in label-free SERS spectra of biofluids reported in literature.

2. Experimental section

2.1. Materials and reagents

All chemicals (analytical grade) for the SERS substrates preparation were purchased from Merck (Darmstadt, Germany) and used as received. L-(+)-ergothioneine (ERG; purity 99.0%) was obtained from NeoBiotech (Nanterre, France). Ultrapure deionized (DI) water of 18.2 MΩ cm resistivity at 25 °C was used throughout the experiments and it was obtained by a Millipore Milli-Q system (Merck, Germany). Phosphate buffered saline (PBS) solution (0.01 M, pH 7.4) was prepared by dissolving one PBS tablet (Sigma-Aldrich) in DI water (200 mL). A standard stock solution (200 μM) of ERG was prepared by dissolving the powder directly in PBS. Fresh working solutions were prepared by diluting the stock solution with PBS to the required concentrations before use. For the preparation of plasmonic paper substrates, qualitative filter paper (grade 410, VWR International, Milan, Italy) with an average pore size of 2 μm has been used.

2.2. Erythrocytes lysates preparation

Blood samples from 3 healthy donors (mean age at enrolment 34 years, 1 male, 2 females) were collected upon informed consent in BD Vacutainer® serum separation tubes from the Transfusion Center of the Azienda Ospedaliera Universitaria of Trieste. Erythrocytes were isolated from whole blood samples by centrifugation for 40 min at 600*g* at 15 °C through a density gradient medium (Ficoll-Paque PLUS, Merck, DE). Dilution 1:1 with distilled water was carried out to obtain lysates, which were subsequently filtered (10 kDa Amicon Ultra 0.5 mL centrifugal filters) at room temperature for 30 min at 14,000 g. All the samples were stored at −80 °C and thawed immediately before data acquisition.

2.3. SERS substrates

Colloidal aqueous dispersions of Ag and Au nanoparticles (NPs) were synthesized according to protocols adapted from Lee-Meisel [15] and Turkevich [16], respectively. Briefly, for Ag-NPs, 45 mg of $AgNO_3$ were dissolved in 250 mL of DI water and heated to boiling. 5 mL of a 1% (wt/v) aqueous sodium citrate tribasic solution were then added dropwise to the $AgNO_3$ solution under vigorous magnetic stirring. The reaction mixture was kept boiling under stirring for 1 h. For Au-NPs, 10.6 mg of $HAuCl_4$ were dissolved in 25 mL DI water, then the solution was heated rapidly with vigorous stirring. When the solution started boiling, 750 mL of a 1% (wt/v) aqueous citrate trisodium solution were added drop by drop. The mixture was boiled for 20 min after the citrate addition. All glassware used for the preparation of both Ag and Au NPs was carefully cleaned with NoChromix® mixture and concentrated solutions of strong acids (aqua regia for Au, HNO_3 for Ag), and then thoroughly rinsed with DI water. Both Au and Ag colloids were stored in the dark at room temperature and were stable for several months. The Ag and Au colloids were characterized by UV–visible absorption spectroscopy using a Cary 60 UV–Vis spectrometer (Agilent Technologies). For AgNPs, the extinction band maxima were between 403, and 406 nm; for AuNPs, the extinction band maxima were between 531 and 540. All these values are consistent with the values previously reported in literature. To obtain Ag plasmonic paper, Ag-NPs have been deposited on a filter paper according to a protocol adapted from Hasi et al. [17] Briefly, 1 cm^2 filter paper squares were pre-treated with a NaCl 1 M aqueous solution for about 20 min to get homogenous imbibition of paper and let it dry. Then, the paper squares were put into a 24 multi-well plate together with 1.5 mL of Ag-NPs colloidal aqueous dispersion. After 24 h, the supernatant was removed, and the sAg-paper substrates let dry. These plasmonic papers were stable up to three months stocked in MilliQ water at dark. Commercial SERS substrates (SERStrates®) comprising of freestanding vertical silicon nanopillars coated with silver were purchased by Silmeco Aps (Copenhagen, Denmark) and used as received.

2.4. Sample preparation for SERS measurements

For the SERS measurements of ERG on colloidal and solid substrates, different procedures have been followed before spectral acquisition. For colloidal substrates, 25 μL of sample solution were mixed with 25 μL of a colloidal dispersion of Ag or Au NPs in a 1.5 mL Eppendorf tube. Immediately after mixing, a change in the colour could be observed, indicating a partial nanoparticle aggregation due to the adsorption of the analytes on the metal surface. The resulting 50 μL drop was rapidly deposited under the microscope objective on a UV-quality grade CaF_2 slide (25 × 75 mm) that was fitted onto the portable microscope stage. A CaF_2 slide has been used to avoid spectral interference from Raman bands or fluorescence from the substrate. Moreover, the low wettability of the CaF_2 surface avoided the spread of the liquid sample, ensuring a thick semi-spherical drop. Ag plasmonic paper substrates were cut into 4 × 4 mm pieces and immersed in the sample solution for 5 min, then thoroughly washed in DI water and sit to let dry at room temperature for about 30 min. For SERStrates, 15 μL of sample solution were deposited onto the substrates surface and let dry at room temperature for about 1 h. The substrates were then rinsed in DI water to remove the excess/unbound molecules. To facilitate handling, all dry solid substrates (Ag plasmonic paper and SERStrates) were placed on a standard microscope slide (25 × 75 mm) that was fitted onto the portable microscope stage before measurements collection. For the SERS measurements of erythrocytes lysates, 5 μL of cell lysate were mixed with 5 μL of Ag colloidal dispersion for a total volume of 10 μL, and placed on CaF_2 slide with a micropipette before collection. Spectra have been collected on the drop after 5 min in order to allow a proper NPs aggregation.

2.5. Instrumentation and spectra collection

Raman and SERS spectra were recorded at room temperature (22 ± 0.5 °C) with a portable i-Raman Plus integrated system (BWS465-785S, B&W Tek, Newark, DE, USA). The instrument was equipped with a CleanLaze® 785 nm laser, tuned to deliver 38–400 mW at the sample, on a spot of about 105 μm in diameter, through the BAC151B Raman Video Micro-sampling System mounting a 20× Olympus objective (working distance 8.8 mm, N.A. 0.25). Instrument settings were

optimised to maximise signal and avoid sample degradation arising from laser excitation. The spectral acquisition was performed with the BWSpec™ version 4.03_23_c (B&W Tek., Newark, DE, USA) software in the Raman shift range 62–3202 cm^{-1}, with an average spectral resolution of 3.22 cm^{-1}, using a 10 s CCD exposure for a single accumulation for SERS spectra and 60 s for Raman spectra. The laser power at the sample was 10% (38 mW) for measurements of ERG solutions, 50% (180 mW) for measurements of erythrocytes lysates and 100% (400 mW) for pure ERG, respectively. The BWSpec™ software allowed to collect a background signal (dark) before data acquisition and to subtract it from collected data. Wavenumber calibration was checked before and during every data collection session by collecting a spectrum from paracetamol as a standard reference. To compensate for intra-substrate variability, three spectra were averaged for each substrate as the final spectrum for that specific sample.

2.6. Data processing and visualization

All data processing and visualization were performed within the R software environment (version 4.0.1 — "See Things Now" [18]) for statistical computing and graphics, building on the package *hyperSpec* [19].

3. Results and discussion

ERG yields intense SERS spectra (Fig. 2) featuring a characteristic strong band at 484 cm^{-1}. While other SERS bands have their corresponding bands in normal Raman spectra (although with substantial wavenumber shifts denoting a strong interaction with the metal), this band is weak or absent in normal Raman spectra of ERG. The high surface enhancement for the corresponding vibrational mode indicates a pivotal role of the molecular moiety involved in the adsorption on the metal surface. In absence of vibrational analysis studies on ERG, a detailed and reliable vibrational assignment of all ERG bands is not possible. However, experimental and theroetical studies detailing a vibrational analysis on structurally related molecules can help in identifying the origin of the band at 484 cm^{-1}. Intense SERS bands between 400 and 500 cm^{-1} have been reported for carbimazole [20], mercaptobenzimidazole [21,22] and methimazole [23–27], suggesting that the heterocyclic moiety bearing the thione group is indeed involved in the adsorption process. In particular, vibrational analyses of methimazole based on DFT studies propose to assign the 500 cm^{-1} band to a N—C—S bending mode mixed with a C—S stretching, suggesting an adsorption mode in which the thiolate anion is forming a bond with the metal, possibly with the involvement of a heterocyclic nitrogen as well [23,24]. On the basis of these studies, we put forward the tentative hypothesis that the thiolate form of ERG is adsorbed on the metal surface via the S and N atoms of its heterocyclic moiety. Further theoretical studies at the DFT level of theory specifically dedicated to ERG are needed to support this hypothesis.

SERS spectra of ERG on colloidal Au are very similar to those obtained on colloidal Ag (Fig. 3), featuring the same spectral pattern (although less intense, all other conditions such as laser power and collection time being the same), and in particular the same intense band around 480 cm^{-1}. Spectra with similar features, with varying absolute intensities, are also observed for ERG on different types of Ag solid substrates (Fig. 4), suggesting that the adsorption mode of this molecule is conserved, irrespective of the metal, substrate type (i.e. colloidal or solid) or other morphological and chemical characteristics (e.g. coating layer). On colloidal Ag (yielding the most intense spectra), ERG gives a linear response in the 0–0.4 μM range (see Supplementary Fig. S1), with a limit of detection of 0.01 μM.

ERG is synthesized by mycobacteria and fungi [3], and bands which can be retrospectively interpreted as due to ERG were indeed reported in SERS spectra of mycobacteria [28] and of some fungi [29,30]. ERG also accumulates in many tissues and biofluids, and SERS spectra from seminal plasma [31,32] and different types of tissues [33–36] can also be retrospectively interpreted as ERG bands.

Since ERG is known to accumulate in erythrocytes [37], we investigated with SERS erythrocytes lysates. The lysates were filtered with a cut-off of 10 kDa to remove hemoglobin molecules as well as other debris (e.g. membranes and other proteins) present as residual from the cell lysis, as these might interfere with nanoparticle aggregation [38]. As expected, SERS spectra of erythrocytes filtered lysates (Fig. 5) are very similar to those of pure ERG solutions (Figs. 2–4), with only minor differences, clearly indicating that the ERG present in the erythrocytes is detected. The fact that other biomolecules that might be present in the filtered lysates are not detected by SERS is not surprising, considering that ERG already yield intense spectra at 100 nM concentration

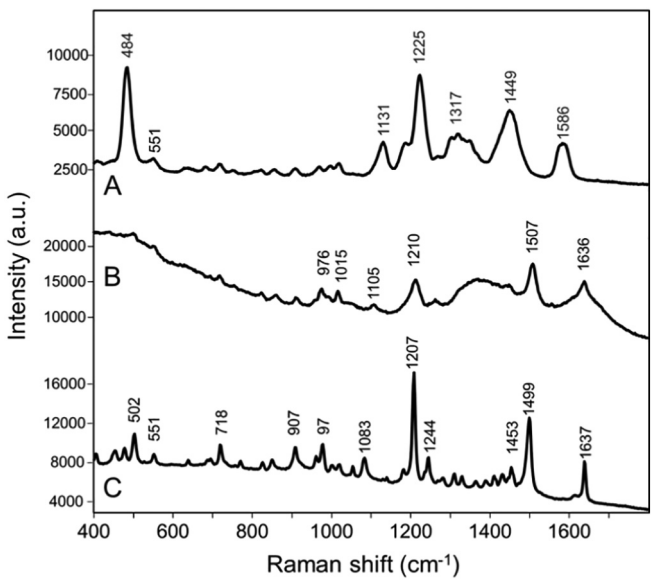

Fig. 2. A: SERS of ERG 0.5 μM on citrate-reduced colloidal Ag; B and C: normal Raman spectra of an aqueous ERG solution (41 mM) and of solid ERG (powder). All spectra were collected with a 785 nm excitation.

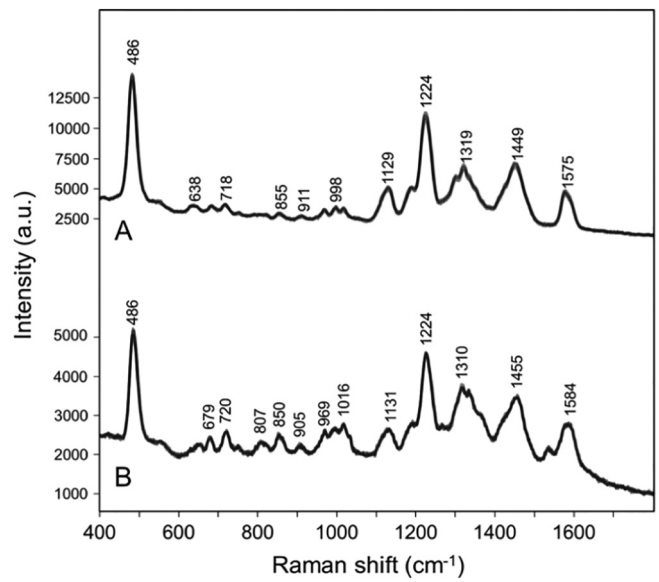

Fig. 3. SERS spectra of ERG 0.1 μM on citrate-reduced colloidal Ag (A) and Au (B). Three technical replicates are shown overlaid for each substrate type. All spectra were collected with a 785 nm excitation.

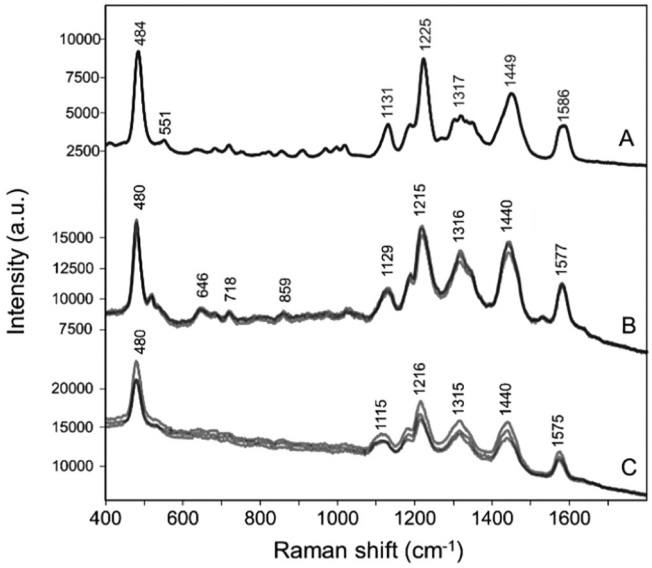

Fig. 4. SERS spectra of ERG 0.5 μM on different Ag substrates: citrate-reduced colloidal Ag (A), Ag on silicon nanopillars (B) and Ag plasmonic paper (C). Three technical replicates are shown overlaid for each substrate type. All spectra were collected with a 785 nm excitation.

(Fig. 3) while in erythrocytes its concentration has been estimated to be about 10^4 times higher (mM) [39,40]. Interestingly, a very recent paper by Shaine et al. also reported SERS spectra of red blood cells lysates which are extremely similar to ours, although they could not identify the origin of the bands [41]. The presence of these intense ERG bands in lysates of red blood cells are likely the reason behind the fact that some authors inadvertently interpreted these bands as due to hemoglobin [42–47]. Since in those studies the hemoglobin was isolated from erythrocytes lysates, a fraction of ERG must have still been present in the samples, together with hemoglobin molecules, after the purification steps. Considering the extremely high concentration of ERG inside red blood cells and its very intense SERS signal, even a 0.01% residual ERG must have been sufficient to yield bands strong enough to overcome those due to hemoglobin (whose SERS spectrum, reported by other authors [48], is noticeably different from that of ERG).

Most importantly, characteristic spectral patterns that can be retrospectively interpreted as due to ERG have been repeatedly reported by different groups in SERS spectra of blood plasma and serum [38,49–56]. This can be explained by the fact that ERG, besides being present in high amounts in red blood cells, has been reported in μM concentrations in plasma as well [6]. In many of these SERS studies on serum and plasma, the characteristic, intense band around 485 cm^{-1}, which can be considered as the most distinctive feature of ERG, has often been misinterpreted as due to L-arginine or glycogen (on the basis of the frequencies observed in that region in normal Raman spectra of these two species). In view of the findings presented in this paper, ERG bands should be considered, together with uric acid and hypoxanthine [57], as one of the main contributors to the SERS spectra of serum and plasma.

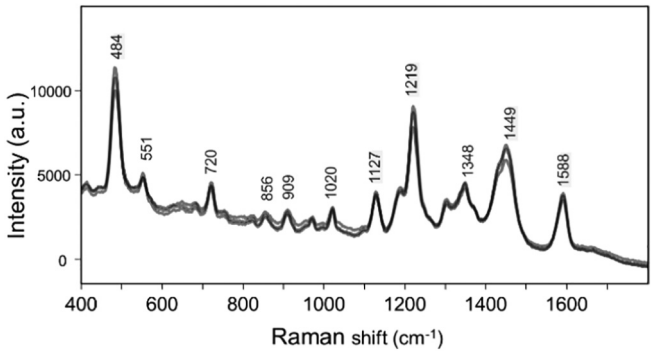

Fig. 5. SERS spectra of filtered erythrocytes lysates on citrate-reduced colloidal Ag. Three replicates from different donors are shown overlaid. All spectra were collected with a 785 nm excitation.

4. Conclusions

ERG yields characteristic, intense SERS spectra on a variety of different substrates, and it is ubiquitously detected in SERS spectra of many tissues and biofluids, in particular in those of serum and plasma where it plays the role of a main spectral component. This finding calls for a retrospective re-interpretation of serum, plasma and hemoglobin SERS spectra reported by different authors in many studies. In perspective, the fact that ERG can be readily detected by SERS even in presence of other species a complex matrix could possibly inspire and guide future studies. Because of its antioxidant properties, a rapid quantitative method based on SERS could be developed to quantify ERG in food and food supplements, or to study its uptake and metabolism *in vitro* or *in vivo*. Moreover, since ERG has been recently reported to be associated with a decreased risk of cardiovascular diseases [10] and of cognitive dysfunctions [14], it might be the target of non-invasive diagnostic and prognostic studies based on label-free SERS of biofluids.

Supplementary data to this article can be found online at https://doi.org/10.1016/j.saa.2020.119024.

CRediT authorship contribution statement

Stefano Fornasaro: Investigation, Visualization, Writing - original draft. **Elisa Gurian:** Investigation, Writing - review & editing. **Sofia Pagarin:** Investigation, Writing - review & editing. **Elena Genova:** Investigation, Writing - review & editing. **Gabriele Stocco:** Supervision, Writing - review & editing. **Giuliana Decorti:** Resources, Writing - review & editing. **Valter Sergo:** Supervision, Resources, Writing - review & editing. **Alois Bonifacio:** Conceptualization, Methodology, Visualization, Writing - original draft.

Declaration of competing interest

The authors declare that they have no known competing financial interests or personal relationships that could have appeared to influence the work reported in this paper.

References

[1] C. Tanret, Sur une base nouvelle retiree du seigle ergote, l'ergothioneine, Rend Acad Sci. 149 (1909) 222–224.
[2] I.K. Cheah, B. Halliwell, Ergothioneine; antioxidant potential, physiological function and role in disease, Biochim. Biophys. Acta (BBA) - Mol. Basis Dis. 1822 (2012) 784–793, https://doi.org/10.1016/j.bbadis.2011.09.017.
[3] I. Borodina, L.C. Kenny, C.M. McCarthy, K. Paramasivan, E. Pretorius, T.J. Roberts, S.A. van der Hoek, D.B. Kell, The biology of ergothioneine, an antioxidant nutraceutical, Nutr. Res. Rev. (2020) 1–28, https://doi.org/10.1017/S0954422419000301.
[4] J. Ey, E. Schömig, D. Taubert, Dietary sources and antioxidant effects of ergothioneine, J. Agric. Food Chem. 55 (2007) 6466–6474, https://doi.org/10.1021/jf071328f.
[5] M.D. Kalaras, J.P. Richie, A. Calcagnotto, R.B. Beelman, Mushrooms: a rich source of the antioxidants ergothioneine and glutathione, Food Chem. 233 (2017) 429–433, https://doi.org/10.1016/j.foodchem.2017.04.109.
[6] I.K. Cheah, R.M.Y. Tang, T.S.Z. Yew, K.H.C. Lim, B. Halliwell, Administration of pure ergothioneine to healthy human subjects: uptake, metabolism, and effects on biomarkers of oxidative damage and inflammation, Antioxid. Redox Signal. 26 (2017) 193–206, https://doi.org/10.1089/ars.2016.6778.

[7] D. Grundemann, S. Harlfinger, S. Golz, A. Geerts, A. Lazar, R. Berkels, N. Jung, A. Rubbert, E. Schomig, Discovery of the ergothioneine transporter, Proc. Natl. Acad. Sci. 102 (2005) 5256–5261, https://doi.org/10.1073/pnas.0408624102.
[8] F. Franzoni, R. Colognato, F. Galetta, I. Laurenza, M. Barsotti, R. Di Stefano, R. Bocchetti, F. Regoli, A. Carpi, A. Balbarini, L. Migliore, G. Santoro, An in vitro study on the free radical scavenging capacity of ergothioneine: comparison with reduced glutathione, uric acid and trolox, Biomed. Pharmacother. 60 (2006) 453–457, https://doi.org/10.1016/j.biopha.2006.07.015.
[9] I.K. Cheah, L. Feng, R.M.Y. Tang, K.H.C. Lim, B. Halliwell, Ergothioneine levels in an elderly population decrease with age and incidence of cognitive decline; a risk factor for neurodegeneration? Biochem. Biophys. Res. Commun. 478 (2016) 162–167, https://doi.org/10.1016/j.bbrc.2016.07.074.
[10] E. Smith, F. Ottosson, S. Hellstrand, U. Ericson, M. Orho-Melander, C. Fernandez, O. Melander, Ergothioneine is associated with reduced mortality and decreased risk of cardiovascular disease, Heart. 106 (2020) 691–697, https://doi.org/10.1136/heartjnl-2019-315485.
[11] R.D. Williamson, F.P. McCarthy, S. Manna, E. Groarke, D.B. Kell, L.C. Kenny, C.M. McCarthy, L-(+)-Ergothioneine significantly improves the clinical characteristics of preeclampsia in the reduced uterine perfusion pressure rat model, Hypertension. 75 (2020) 561–568, https://doi.org/10.1161/HYPERTENSIONAHA.119.13929.
[12] O. Sakrak, M. Kerem, A. Bedirli, H. Pasaoglu, N. Akyurek, E. Ofluoglu, F.A. Gültekin, Ergothioneine modulates proinflammatory cytokines and heat shock protein 70 in mesenteric ischemia and reperfusion injury, J. Surg. Res. 144 (2008) 36–42, https://doi.org/10.1016/j.jss.2007.04.020.
[13] J.E. Repine, N.D. Elkins, Effect of ergothioneine on acute lung injury and inflammation in cytokine insufflated rats, Prev. Med. 54 (2012) S79–S82, https://doi.org/10.1016/j.ypmed.2011.12.006.
[14] M. Kameda, T. Teruya, M. Yanagida, H. Kondoh, Frailty markers comprise blood metabolites involved in antioxidation, cognition, and mobility, Proc. Natl. Acad. Sci. 117 (2020) 9483–9489, https://doi.org/10.1073/pnas.1920795117.
[15] P.C. Lee, D. Meisel, Adsorption and surface-enhanced Raman of dyes on silver and gold sols, J. Phys. Chem. 86 (1982) 3391–3395, https://doi.org/10.1021/j100214a025.
[16] J. Kimling, M. Maier, B. Okenve, V. Kotaidis, H. Ballot, A. Plech, Turkevich method for gold nanoparticle synthesis revisited, J. Phys. Chem. B 110 (2006) 15700–15707, https://doi.org/10.1021/jp061667w.
[17] W.-L.-J. Hasi, X. Lin, X.-T. Lou, S. Lin, F. Yang, D.-Y. Lin, Z.-W. Lu, Chloride ion-assisted self-assembly of silver nanoparticles on filter paper as SERS substrate, Appl. Phys. A Mater. Sci. Process. 118 (2014) 799–807, https://doi.org/10.1007/s00339-014-8800-x.
[18] R Core Team, R: A Language and Environment for Statistical Computing, R Found. Stat. Comput. https://www.R-project.org/ 2020.
[19] C. Beleites, V. Sergo, HyperSpec: A Package to Handle Hyperspectral Data Sets in R, R Package Version 099-20200527, https://github.com/cbeleites/hyperSpec 2020.
[20] X. Bu, Z. Zhang, L. Zhang, P. Li, J. Wu, H. Zhang, Y. Tian, Highly sensitive SERS determination of chromium(VI) in water based on carbimazole functionalized alginate-protected silver nanoparticles, Sensors Actuators B Chem. 273 (2018) 1519–1524, https://doi.org/10.1016/j.snb.2018.07.058.
[21] H.L. Zheng, S.S. Yang, J. Zhao, Z.C. Zhang, Synthesis of rGO–Ag nanoparticles for high-performance SERS and the adsorption geometry of 2-mercaptobenzimidazole on Ag surface, Appl. Phys. A Mater. Sci. Process. 114 (2013) 801–808, https://doi.org/10.1007/s00339-013-7659-6.
[22] S.M. Ansar, R. Haputhanthri, B. Edmonds, D. Liu, L. Yu, A. Sygula, D. Zhang, Determination of the binding affinity, packing, and conformation of thiolate and thione ligands on gold nanoparticles, J. Phys. Chem. C 115 (2010) 653–660, https://doi.org/10.1021/jp110240y.
[23] M. Muniz-Miranda, F. Muniz-Miranda, A. Pedone, Raman and DFT study of methimazole chemisorbed on gold colloidal nanoparticles, Phys. Chem. Chem. Phys. 18 (2016) 5974–5980, https://doi.org/10.1039/c5cp07597a.
[24] T.A. Saleh, M.M. Al-Shalalfeh, A.A. Al-Saadi, Silver nanoparticles for detection of methimazole by surface-enhanced Raman spectroscopy, Mater. Res. Bull. 91 (2017) 173–178, https://doi.org/10.1016/j.materresbull.2017.03.041.
[25] X. Liao, Y. Chen, M. Qin, Y. Chen, L. Yang, H. Zhang, Y. Tian, Au–Ag–Au double shell nanoparticles-based localized surface plasmon resonance and surface-enhanced Raman scattering biosensor for sensitive detection of 2-mercapto-1-methylimidazole, Talanta. 117 (2013) 203–208, https://doi.org/10.1016/j.talanta.2013.08.051.
[26] R. Zhang, Y. Wen, N. Wang, Y. Wang, Y. Wang, Z. Zhang, H. Yang, Insight in the relationship between the structure and property of methimazole monolayers on a silver surface: electrochemical and Raman study, J. Phys. Chem. B 114 (2010) 2450–2456, https://doi.org/10.1021/jp911024d.
[27] N. Biswas, S. Thomas, A. Sarkar, T. Mukherjee, S. Kapoor, Adsorption of methimazole on silver nanoparticles: FTIR, Raman, and surface-enhanced Raman scattering study aided by density functional theory, J. Phys. Chem. C 113 (2009) 7091–7100, https://doi.org/10.1021/jp900134n.
[28] T.-Y. Liu, J.-Y. Ho, J.-C. Wei, W.-C. Cheng, I.H. Chen, J. Shiue, H.-H. Wang, J.-K. Wang, Y.-L. Wang, J.-J. Lin, Label-free and culture-free microbe detection by three dimensional hot-junctions of flexible Raman-enhancing nanohybrid platelets, J. Mater. Chem. B 2 (2014) 1136–1143, https://doi.org/10.1039/c3tb21469a.
[29] E. Witkowska, T. Jagielski, A. Kamińska, A. Kowalska, A. Hryncewicz-Gwóźdź, J. Waluk, Detection and identification of human fungal pathogens using surface-enhanced Raman spectroscopy and principal component analysis, Anal. Methods 8 (2016) 8427–8434, https://doi.org/10.1039/c6ay02957d.
[30] E. Witkowska, T. Jagielski, A. Kamińska, Genus- and species-level identification of dermatophyte fungi by surface-enhanced Raman spectroscopy, Spectrochim. Acta A Mol. Biomol. Spectrosc. 192 (2018) 285–290, https://doi.org/10.1016/j.saa.2017.11.008.
[31] Z. Huang, G. Cao, Y. Sun, S. Du, Y. Li, S. Feng, J. Lin, J. Lei, Evaluation and optimization of paper-based SERS substrate for potential label-free Raman analysis of seminal plasma, J. Nanomater. 2017 (2017) 1–8, https://doi.org/10.1155/2017/4807064.
[32] X. Chen, Z. Huang, Feng, J.H. Chen, Wang, Lu, H. Zeng, Chen, Analysis and differentiation of seminal plasma via polarized SERS spectroscopy, Int. J. Nanomedicine (2012)https://doi.org/10.2147/ijn.S37782.
[33] S. Feng, J. Lin, M. Cheng, Y.-Z. Li, G. Chen, Z. Huang, Y. Yu, R. Chen, H. Zeng, Gold nanoparticle based surface-enhanced Raman scattering spectroscopy of cancerous and normal nasopharyngeal tissues under near-infrared laser excitation, Appl. Spectrosc. 63 (2009) 1089–1094, https://doi.org/10.1366/000370209789553291.
[34] S. Cinta Pinzaru, C.A. Dehelean, A. Falamas, N. Leopold, C. Lehene, Cancer tissue screening using surface enhanced Raman scattering, Proc. SPIE 7376 (2010) 73760T, https://doi.org/10.1117/12.871378.
[35] S. Feng, J. Lin, Z. Huang, G. Chen, W. Chen, Y. Wang, R. Chen, H. Zeng, Esophageal cancer detection based on tissue surface-enhanced Raman spectroscopy and multivariate analysis, Appl. Phys. Lett. 102 (2013)https://doi.org/10.1063/1.4789996.
[36] A. Falamas, C.A. Dehelean, S. Cinta Pinzaru, Monitoring of betulin nanoemulsion treatment and molecular changes in mouse skin cancer using surface enhanced Raman spectroscopy, Vib. Spectrosc. 95 (2018) 44–50, https://doi.org/10.1016/j.vibspec.2018.01.004.
[37] B. Halliwell, I.K. Cheah, R.M.Y. Tang, Ergothioneine - a diet-derived antioxidant with therapeutic potential, FEBS Lett. 592 (2018) 3357–3366, https://doi.org/10.1002/1873-3468.13123.
[38] A. Bonifacio, S. Dalla Marta, R. Spizzo, S. Cervo, A. Steffan, A. Colombatti, V. Sergo, Surface-enhanced Raman spectroscopy of blood plasma and serum using Ag and Au nanoparticles: a systematic study, Anal. Bioanal. Chem. 406 (2014) 2355–2365, https://doi.org/10.1007/s00216-014-7622-1.
[39] H. Mitsuyama, J.M. May, Uptake and antioxidant effects of ergothioneine in human erythrocytes, Clin. Sci. 97 (1999) 407–411.
[40] T.A. Kumosani, L-ergothioneine level in red blood cells of healthy human males in the Western province of Saudi Arabia, Exp. Mol. Med. 33 (2001) 20–22, https://doi.org/10.1038/emm.2001.4.
[41] M.L. Shaine, W.R. Premasiri, H.M. Ingraham, R. Andino, P. Lemler, A.N. Brodeur, L.D. Ziegler, Surface enhanced Raman scattering for robust, sensitive detection and confirmatory identification of dried bloodstains, Analyst 145 (2020) 6097–6110, https://doi.org/10.1039/D0AN01132K.
[42] Y. Kang, M. Si, R. Liu, S. Qiao, Surface-enhanced Raman scattering (SERS) spectra of hemoglobin on nano silver film prepared by electrolysis method, J. Raman Spectrosc. 41 (2010) 614–617, https://doi.org/10.1002/jrs.2489.
[43] Y. Kang, M. Si, Y. Zhu, L. Miao, G. Xu, Surface-enhanced Raman scattering (SERS) spectra of hemoglobin of mouse and rabbit with self-assembled nano-silver film, Spectrochim Acta Mol Biomol Spectrosc. 108 (2013) 177–180, https://doi.org/10.1016/j.saa.2013.01.098.
[44] R. Liu, M. Si, Y. Kang, X. Zi, Z. Liu, D. Zhang, A simple method for preparation of Ag nanofilm used as active, stable, and biocompatible SERS substrate by using electrostatic self-assembly, J. Colloid Interface Sci. 343 (2010) 52–57, https://doi.org/10.1016/j.jcis.2009.11.042.
[45] R. Liu, Y. Xiong, W. Tang, Y. Guo, X. Yan, M. Si, Near-infrared surface-enhanced Raman spectroscopy (NIR-SERS) studies on oxyheamoglobin (OxyHb) of liver cancer based on PVA-Ag nanofilm, J. Raman Spectrosc. 44 (2013) 362–369, https://doi.org/10.1002/jrs.4216.
[46] J. Lin, Z. Huang, S. Feng, J. Lin, N. Liu, J. Wang, L. Li, Y. Zeng, B. Li, H. Zeng, R. Chen, Label-free optical detection of type II diabetes based on surface-enhanced Raman spectroscopy and multivariate analysis, J. Raman Spectrosc. 45 (2014) 884–889, https://doi.org/10.1002/jrs.4574.
[47] D. Drescher, T. Büchner, D. McNaughton, J. Kneipp, SERS reveals the specific interaction of silver and gold nanoparticles with hemoglobin and red blood cell components, Phys. Chem. Chem. Phys. 15 (2013)https://doi.org/10.1039/c3cp43883j.
[48] X.X. Han, G.G. Huang, B. Zhao, Y. Ozaki, Label-free highly sensitive detection of proteins in aqueous solutions using surface-enhanced Raman scattering, Anal. Chem. 81 (2009) 3329–3333, https://doi.org/10.1021/ac900395x.
[49] X. Li, T. Yang, S. Li, L. Jin, D. Wang, D. Guan, J. Ding, Noninvasive liver diseases detection based on serum surface enhanced Raman spectroscopy and statistical analysis, Opt. Express 23 (2015) 18361–18372, https://doi.org/10.1364/OE.23.018361.
[50] H. Jin, Q. Lu, S. Jin, Z. Song, Y. Zou, H. Ding, H. Gao, X. Chen, Research on measurement conditions for obtaining significant, stable, and repeatable SERS signal of human blood serum, IEEE Photonics J. 9 (2017) 1–10, https://doi.org/10.1109/jphot.2017.2672900.
[51] S. Feng, R. Chen, J. Lin, J. Pan, G. Chen, Y. Li, M. Cheng, Z. Huang, J. Chen, H. Zeng, Nasopharyngeal cancer detection based on blood plasma surface-enhanced Raman spectroscopy and multivariate analysis, Biosens. Bioelectron. 25 (2010) 2414–2419, https://doi.org/10.1016/j.bios.2010.03.033.
[52] J. Li, J. Ding, X. Liu, B. Tang, X. Bai, Y. Wang, S. Li, X. Wang, Label-free serum detection of Trichinella spiralis using surface-enhanced Raman spectroscopy combined with multivariate analysis, Acta Trop. 203 (2020)https://doi.org/10.1016/j.actatropica.2019.105314.
[53] D. Lin, Y. Wang, T. Wang, Y. Zhu, X. Lin, Y. Lin, S. Feng, Metabolite profiling of human blood by surface-enhanced Raman spectroscopy for surgery assessment and tumor screening in breast cancer, Anal. Bioanal. Chem. 412 (2020) 1611–1618, https://doi.org/10.1007/s00216-020-02391-4.
[54] Y. Lu, Y. Lin, Z. Zheng, X. Tang, J. Lin, X. Liu, M. Liu, G. Chen, S. Qiu, T. Zhou, Y. Lin, S. Feng, Label free hepatitis B detection based on serum derivative surface enhanced Raman spectroscopy combined with multivariate analysis, Biomed. Opt. Express. 9 (2018)https://doi.org/10.1364/boe.9.004755.

[55] R. Liu, Y. Xiong, Y. Guo, M. Si, W. Tang, Label-free and non-invasive BS-SERS detection of liver cancer based on the solid device of silver nanofilm, J. Raman Spectrosc. 49 (2018) 1426–1434, https://doi.org/10.1002/jrs.5408.
[56] Q. Wu, S. Qiu, Y. Yu, W. Chen, H. Lin, D. Lin, S. Feng, R. Chen, Assessment of the radiotherapy effect for nasopharyngeal cancer using plasma surface-enhanced Raman spectroscopy technology, Biomed. Opt. Express. 9 (2018)https://doi.org/10.1364/boe.9.003413.
[57] A. Bonifacio, S. Cervo, V. Sergo, Label-free surface-enhanced Raman spectroscopy of biofluids: fundamental aspects and diagnostic applications, Anal. Bioanal. Chem. 407 (2015) 8265–8277, https://doi.org/10.1007/s00216-015-8697-z.